Published in final edited form as:
Arterioscler Thromb Vasc Biol. 2012 April ; 32(4): 962–970. doi:10.1161/ATVBAHA.111.244509.

In Vivo Targeting of Inflammation-Associated Myeloid-Related Protein 8/14 Via Gadolinium Immunonanoparticles

Andrei Maiseyeu
Davis Heart & Lung Research Institute, The Ohio State University College of Medicine, Columbus, OH

Marcus A. Badgeley
Davis Heart & Lung Research Institute, The Ohio State University College of Medicine, Columbus, OH

Thomas Kampfrath
Davis Heart & Lung Research Institute, The Ohio State University College of Medicine, Columbus, OH

Georgeta Mihai
Davis Heart & Lung Research Institute, The Ohio State University College of Medicine, Columbus, OH

Jeffrey A. Deiuliis
Davis Heart & Lung Research Institute, The Ohio State University College of Medicine, Columbus, OH

Cuiqing Liu
Davis Heart & Lung Research Institute, The Ohio State University College of Medicine, Columbus, OH

Qinghua Sun
Division of Environmental Health Sciences, The Ohio State University College of Public Health, Columbus, OH

Sampath Parthasarathy
Burnett School of Biomedical Sciences, University of Central Florida, Orlando, FL

Daniel I. Simon
University Hospitals Case Medical Center, Case Cardiovascular Center, Case Western Reserve University School of Medicine, Cleveland, OH

Kevin Croce
Donald W. Reynolds Cardiovascular Clinical Research Center, Department of Medicine, Brigham and Women's Hospital, Harvard Medical School, Boston, MA

Sanjay Rajagopalan
Davis Heart & Lung Research Institute, The Ohio State University College of Medicine, Columbus, OH

Abstract

Correspondence to Sanjay Rajagopalan, Davis Heart & Lung Research Institute, 473 W. 12th Avenue, Room 110, Columbus, OH 43210. Sanjay.Rajagopalan@osumc.edu.

Disclosures None.

Objective—Myeloid-related protein (Mrp) 8/14 complex (is a highly expressed extracellularly secreted protein, implicated in atherosclerosis. In this study, we evaluated the feasibility of targeting Mrp in vivo through synthetic immunonanoprobes.

Methods and Results—Anti-Mrp-14 and nonspecific IgG-conjugated gadolinium nanoprobes (aMrp-) were synthesized and characterized. Pharmacokinetics and vascular targeting via MRI of the formulations were assessed in vivo in high fat-fed apolipoprotein E deficient ($ApoE^{-/-}$), $ApoE^{-/-}/Mrp14^{-/-}$ (double knockout) and chow-fed wild-type (C57BL/6) mice. Bone marrow-derived myeloid progenitor cells were isolated from both $ApoE^{-/-}$ and double knockout mice, differentiated to macrophages, and were treated with LPS, with or without Mrp8, Mrp14, or Mrp8/14; conditioned media was used for in vitro studies. Mrp-activated cells secreted significant amounts of proinflammatory cytokines, which was abolished by pretreatment with aMrp-NP. We show in vitro that aMrp-NP binds endothelial cells previously treated with conditioned media containing Mrp8/14. MRI following intravenous delivery of aMrp-NP revealed prolonged and substantial delineation of plaque in $ApoE^{-/-}$ but not double knockout or wild-type animals. Nonspecific IgG-conjugated gadolinium nanoprobe-injected animals in all groups did not show vessel wall enhancement. Flow-cytometric analysis of aortic digesta revealed that aMrp-NP present in $Ly\text{-}6G^{+}$, $CD11b^{+}$, $CD11c^{+}$, and $CD31^{+}$ cells in $ApoE^{-/-}$ but not in double knockout animals.

Conclusion—Targeted imaging with aMrp-NP demonstrates enhancement of plaque with binding to inflammatory cells and reduction in inflammation. This strategy has promise as a theranostic approach for atherosclerosis.

Keywords

atherosclerosis; imaging agents; macrophages; magnetic resonance imaging

Myeloid-related protein (Mrp)-8/14 is a member of the S100-family of Ca^{2+}-modulated proteins. Mrp exists as a heterodimer of Mrp-14 (S100A9 or calgranulin B) and Mrp-8 (S100A8 or calgranulin A), with prior studies demonstrating an important role for the Mrp complex in the inflammatory response to injury.[1] Mrp has been shown to exert potent proinflammatory effects through activation of innate immune pathways including Toll-like receptor-4 (TLR-4) and receptor of advanced glycation end-products.[1–6] Studies in Mrp-14 deficient ($Mrp\text{-}14^{-/-}$) mice indicate that this molecule broadly regulates vascular inflammation in atherosclerosis, vasculitis, and experimental angioplasty.[1,2,7] Mrp-8/14 is found predominantly in the cytoplasm of resting neutrophils and monocytes and is rapidly secreted in response to activation.[4,8] Mrp8/14 is abundantly detected in human and mouse atherosclerotic plaques and colocalizes to rupture prone areas of plaque typified by large necrotic cores and high macrophage content. Indeed, a subset of macrophages expressing Mrp have been demonstrated in human atherosclerosis and predominate in rupture-prone lesions compared to stable plaques.[5] Consistent with its extracellular abundance and signaling, levels of Mrp have been shown to independently prognosticate cardiovascular risk.[7]

We have previously shown that nanoparticles incorporating a widely expressed lipid within foam cells (ω-carboxynonanoyl-cholesteryl ester) serves as a potent engulfment signal and is avidly taken up by plaque macrophages.[9] We and others have also demonstrated that the routine incorporation of phosphatidylserine (PS) in nanoparticles has the further advantage of exerting anti-inflammatory effects on plaque macrophages besides demonstrating favorable pharmacokinetic properties and stability.[9–11] In this investigation, we synthesized multivalent theranostic nanoparticles composed of PS, ω-carboxynonanoyl-cholesteryl ester, and gadolinium lipids which were additionally coupled with anti-Mrp14 polyclonal antibody (aMrp-NP). We hypothesized that targeting inflammatory regions of plaque with aMrp-NP

will allow imaging of inflammation in a locus specific manner, in addition to exerting anti-inflammatory effects. Our choice of Mrp as a target for theranostic imaging was predicated by the following characteristics: (1) high expression in inflammatory plaques and may enable delivery of high contrast doses; (2) participation in proinflammatory cascades; and (3) active secretion and binding to both cell surface and the extracellular matrix in inflamed plaque that may facilitate prolonged tissue retention of diagnostic probe.

Methods

Nanoprobe Synthesis and Characterization

A schematic overview of design and synthesis is given in Figure 1. The overall synthesis was achieved in 3 separate steps. Near-infrared dye labeled lipids were synthesized by coupling commercially available NHS-activated AlexaFluor-647 dye and phosphoethanolamine. Gadolinium lipids (Gd-DTPA-BSA) were synthesized as described previously.[9,10] Pegylated lipids (DSPE-PEG) as well as maleimide-labeled PEG lipids were incorporated into the formulation, in order to provide longer blood half-life and enable antibody attachment. Additionally phosphatidylserine, ω-carboxynonanoylcholesteryl ester,[9] and phosphatidylcholine were incorporated into the nanoparticles, which were then used for antibody conjugation. To synthesize immuno-nanoparticles targeted to Mrp (aMrp-NP), we first labeled commercially available polyclonal goat antimouse Mrp14 with conjugation reagent SATP. Hydroxylamine treatment cleaved acetyl group in SATP-tagged antibody providing a free sulfhydryl moiety. Maleimide-sulfhydryl chemistry covalently linked anti-Mrp14 to the surface of the nanoparticle. Nonspecific nanoparticles displaying polyclonal human immunoglobulin on their surface (nonspecific IgG-conjugated gadolinium nanoprobe [IgG-NPs]) were synthesized in a similar manner. Details of each step as well as physicochemical characterization of nanoprobes can be found in online-only Data Supplement.

Animal Models

The male ApoE$^{-/-}$ (n=10) and C57BL/6 (n=3) mice were obtained from Jackson Laboratories (Bar Harbor, ME). Twelve male age-matched ApoE$^{-/-}$/Mrp14$^{-/-}$ (double knockout [DKO]) were provided by Dr. K. Croce (Brigham and Women's Hospital, Boston, MA). All animals were placed on a high-fat/high-cholesterol diet (0.2% total cholesterol, 42% calories from fat; Harlan Teklad, Madison, WI) ad libitum beginning at 17 weeks until 37 weeks of age. The Committee on Use and Care of Animals from the Ohio State University (OSU) approved all experimental procedures.

In Vivo MRI

In vivo MRI scans were performed using a 11.7 T Bruker BioSpin MRI System (Billerica, MA) as previously described.[10] Acquisition parameters optimized to depict the aortic wall were set as following: twelve 0.1×0.1×0.5 mm^3 transversal contiguous slices, TR/TE=316/3.7 ms, flip angle=20, four averages. Images were analyzed using OsiriX software as described in online-only Data Supplement.

In Vitro Experiments in Bone Marrow Derived Macrophages

Bone marrow was isolated from ApoE$^{-/-}$ and DKO mice by flushing the femurs and tibias with PBS plus 5% FBS. Cells were cultured as previously described in 150 mm suspension culture dishes until differentiation into macrophages (bone marrow derived macrophages [BMDM]).[12] The macrophages thus obtained were then plated in 24-well or in 6-well plates containing glass coverslips at a density of 2×10^5 and 1×10^6 cells/well, respectively. Cells were then stimulated with 1 μg/mL LPS (Sigma) or 2.5 μg/mL recombinant Mrp8 and/or

Mrp14 (both from Novus Biologicals) in the presence or absence of 25 μg/mL polymyxin B (Sigma), 0.1 mmol/L aMrp-NP, IgG-NP, or sham (PBS or bare particles) for 4 hours at 37°C. In 1 experiment, recombinant Mrp proteins were deactivated by heating in a boiling water bath for 30 minutes. After treatment, supernatants were collected and assayed for cytokine release using either TNF-α ELISA kit (R&D Systems) or BD cytometric bead array mouse inflammation 6-plex kit (BD Bioscience, CA). To obtain cell-conditioned media (CM) from activated cells, 20 to 30×10^6 cells were challenged with 1 μg/mL LPS for 5 hours, washed with PBS two times and continued to culture in 25 mL complete media for additional 24 hours. Resulting CM was concentrated to 5 mL with Centricon-30 centrifuge filters (Millipore) and used in endothelial cell binding assays.

Endothelial Cell Binding Assays

Human umbilical vein endothelial cells (HUVECs, Invitrogen) were maintained in medium 199 (Invitrogen) supplemented with a brain bovine extract (Lonza) and 20% FBS according to vendor's directions. All experiments were conducted with confluent cultures of cells in H-HBSS binding buffer consisting of Hank's buffered salt solution (HBSS) with 25 mmol/L HEPES, 0.2% BSA, 1 mmol/L $CaCl_2$, 1 mmol/L $MgSO_4$, and 10 μmol/L $ZnSO_4$.[13] The cells either in suspension (2×10^6) or bound to glass coverslips were incubated on ice for 40 minutes with rMrp8/14, or DKO/ApoE$^{-/-}$ CM and then washed 3 times with H-HBSS. Next, the cells were resuspended in 100 μL of H-HBSS containing 0.1 mmol/L of either aMrp-NP or IgG-NP and incubated on ice for 30 minutes. The cells bound to coverslips were treated by direct addition of 0.1 mmol/L particles in H-HBSS onto coverslip. After washing, the cells were then fixed in PBS +2% formaldehyde and analyzed by flow cytometry or stained with 4′,6-diamidino-2-phenylindole (DAPI) followed by imaging on Olympus FV1000 spectral confocal microscope.

In Vivo Cellular Selectivity Profiling of aMrp-NP

Thirty to 36 hours after aMrp-NP injection and following MRI scans, animals were euthanized and whole aortas were isolated. The aortas were dissected and incubated in 2 mL of 25 mmol/L HEPES-buffered enzyme cocktail for 1 hour with gentle shaking. The enzyme mix consisted of 600 U/mL Collagenase XI, 1500 U/mL Collagenase I, 400 kU/mL DNAse I, and 500 U/mL Hyaluronidase (all from Sigma). Aortic digesta were passed through a 70-μm cell strainer (Falcon) and cells were pelleted via centrifugation. Next, the cell pellets were treated with 1 mL of red blood cell lysis buffer (Qiagen) for 1 minute at room temperature followed by the addition of 14 mL of PBS. After pelleting, the cells were resuspended in FACS buffer (5% FBS in PBS) and washed twice, followed by incubation with anti-CD90.2 (Thy-1.2), anti-CD45R/B220, anti-Ly-6G, anti-CD11b, anti-CD11c, and anti-CD31 antibodies (labeled with Pacific blue, AlexaFluor 488, APC/Cy7, PE/Cy5, PE/Cy7, and PE, respectively; all from Biolegend, San Diego, CA) for 1 hour. Cells were subsequently washed with FACS buffer, resuspended in 1% formalin, and analyzed using a BD FACS LSR II flow cytometer (Becton Dickinson, San Jose, CA).

Statistics

Data are expressed as mean±SEM. Multiple measures ANOVA was used to compare imaging results before and after aMrp-NP injection. An unpaired *t* test was used to compare the difference between treatment conditions in cell culture experiments. Statistical significance was accepted at $P<0.05$.

Results

Synthesis of Anti-Mrp14–Directed Nanoparticles and Their Physicochemical Properties

Figure 1 demonstrates an overview of the nanoparticle synthesis. The mean size of the nanoparticles was 83 nm for aMrp-NPs and 96 nm for IgG-NPs as was determined by dynamic light scattering (Figure IA in the online-only Data Supplement). Longitudinal relaxation values (r1) obtained at 1.5 T (Figure IB in the online-only Data Supplement) were similar in both formulations (6.2±1.8 and 6±1 $s^{-1} \cdot mM^{-1}$). Fluorescence spectra recorded for immunonanoparticles indicated that the amount of fluorescent AlexaFluor 647 was equal in both formulations (Figure IC in the online-only Data Supplement).

Single-dose time-dependent studies using aMrp-NP and IgG-NP demonstrated that both were taken up avidly by RAW cells (Figure IIA in the online-only Data Supplement). Furthermore, confocal microscopy imaging showed distinct colocalization of AlexaFluor 647 with LAMP1, indicating localization of the nanoparticles to the lysosomal compartment (Figure IIB and IIC in the online-only Data Supplement).

We investigated whether in vivo circulating nanoparticles are intact. We subjected the serum isolated from animals injected with aMrp-NP (serum-aMrp-NP) to FPLC. Pure aMrp-NP served as control. For each FPLC fraction we recorded absorption at 280 nm (indicate the presence of proteins) and fluorescence emission at 665 nm on excitation at 647 nm (AF647 fluorescence of nanoparticles). Corresponding FPLC chromatograms are shown in Figure IID and IIE in the online-only Data Supplement. Absorption and fluorescence emission peaks merge in aMrp-NP, whereas there is a fluorescence peak shift in serum-aMrp-NP indicating some lipid exchange between nanoparticles and serum constituents (eg, lipoproteins). This data also suggests that a large portion of nanoparticles still remains intact as seen by the presence of original aMrp-NP peaks at fractions 12 to 20.

In Vivo Plaque Imaging Characteristics of Gd-Containing aMrp-NP

The in vivo imaging efficiency of Gd-containing aMrp-NP was investigated in high-fat fed $ApoE^{-/-}$ and $ApoE^{-/-}/Mrp14^{-/-}$ (DKO) mouse models of experimental atherosclerosis. Immunohistochemistry confirmed the presence of Mrp in $ApoE^{-/-}$ but not in DKO mice (Figure III in the online-only Data Supplement). Figure 2A depicts representative MRI images of the abdominal aorta from $ApoE^{-/-}$ and DKO animals obtained 24 hours following injection of aMrp-NP. There was approximately a ≈5-fold increase in enhancement of the aortic wall compared to muscle with aMrp-NP in $ApoE^{-/-}$ (Figure IV in the online-only Data Supplement). In contrast the DKO animals demonstrated no enhancement. Figure 2C depicts the contrast to noise ratio in $ApoE^{-/-}$ compared to DKO animals. Contrast-to-noise ratio aMrp-NP administration increased ≈22-fold in $ApoE^{-/-}$ animals compared to no significant change in the DKO animals. These changes were observed in the absence of any effect on the signal-to-noise ratio of muscle in both the animal groups (Figure 2C). It could be argued that the reduced signal noted in the DKO animals may reflect attenuation in plaque as has been demonstrated previously.[1] Prominent atherosclerotic was still noted in the DKO animals (Figure VA and VB in the online-only Data Supplement). Moreover, nonatherosclerotic chow-fed animals (C57BL/6) did not exhibit aortic wall enhancement after aMrp-NP injection (Figure VI in the online-only Data Supplement) suggesting specificity of aMrp-NP to inflammatory atherosclerotic vessels. Because of fast clearance of nanoparticles from circulation (Figure 3), absence of lipid-laden plaques, and lack of expression of Mrp in the vessel wall, the C57BL/6 mice did not show any nonspecific accumulation of aMrp-NP.

Histological Validation, Pharmacokinetics and Biodistribution of aMrp-NP

Adjacent aortic sections were analyzed by confocal microscopy as well as stained with antibodies against F4/80 (Figure 3A). Specificity of aMrp-NP staining was confirmed by acquisition of fluorescent images in FITC channel, whereas F4/80 specificity was determined with control IgG antibody. Intensive AF647 fluorescent signal was registered in ApoE$^{-/-}$ mice but not in DKO mice, which also colocalized with F4/80 positive cells. The pharmacokinetic profiles of aMrp-NP revealed a half-life of ≈17 and 32 minutes in ApoE$^{-/-}$ and DKO mice respectively (Figure 3B). The more rapid clearance of aMrp-NP seen in ApoE$^{-/-}$ may relate to its avid uptake by cell populations that express Mrp including within atherosclerotic plaque. The nanoparticles preferentially accumulated in RES organs (liver and spleen) in both models, with the extent of accumulation being no different between ApoE$^{-/-}$ versus DKO animals (Figure 3C). We then proceeded to assess the targeting specificity of aMrp-NP to cells prevalent within the atherosclerotic plaque.

Targeting Selectivity of aMrp-NPs in Atherosclerosis

Flow-cytometric assessment of cell populations from aortic plaque digestates from ApoE$^{-/-}$ and DKO animals identified accumulation of aMrp-NP in CD11b^{+} cells that may include monocytes/macrophages/neutrophils (aMrp-NP^{+}/CD11b^{hi}), granulocytes/neutrophils (aMrp-NP^{+}/Ly6G^{hi}), and endothelial cells (aMrp-NP^{+}/CD31^{+}) as the predominant cellular targets for aMrp-NP (Figure 4A, B). Notably, DKO mice had markedly reduced binding of aMrp-NP consistent with targeting specificity (Figure 4A). Some uptake of aMrp-NPs was also seen in B-cells (CD45/B220^{+}) and in cells expressing CD11c, considered to be a marker for macrophage/dendritic cell populations (CD11c^{+}). This is consistent with previously reported Mrp content in these cell populations.[14] In light of a high-degree of binding to endothelial cells in our in vivo studies, we speculated that the Mrp-8/14 complex binds to components of the endothelium and/or extracellular matrix.[13,15] To further support our hypothesis, we performed additional in vitro experiments in cultured HUVEC cells.

Exogenous Myeloid-Related Proteins Exaggerate aMrp-NP Binding to Endothelial Cells

In the first experiment, HUVECs were treated with mixture of recombinant Mrp8 and Mrp14 or GST control. In another experiment, treatment was performed with cell-conditioned CM of LPS-activated BMDMs from either ApoE$^{-/-}$ or DKO mice. aMrp-NP or IgG-NP was added 30 minutes after treatment and AlexaFluor 647 staining was detected by flow-cytometry or confocal microscopy (Figure 5A and 5B). The results demonstrated that HUVECs treated with either rMrp8/14 or ApoE$^{-/-}$ CM accumulated large amounts of aMrp-NP on their surface. In contrast, sham- or DKO CM-treated cells were minimally stained with AlexaFluor 647, which may reflect engulfment of nanoparticles via endocytosis. As anticipated, nonspecific immunoglobulin-modified probes IgG-NPs did not possess Mrp specificity, which was evident in both sets of experiments. These in vitro results were confirmed by immunofluorescence analysis in aortic sections. Distinctive costaining of heparan sulfate and aMrp-NP was evident in ApoE$^{-/-}$. However in the DKO, this distinct pattern of intramembranous staining was no longer seen, with the staining acquiring a discrete perimembranous appearance (Figure VII in the online-only Data Supplement). Additionally, we investigated whether circulating aMrp-NPs retain their heparin binding properties (Figure VIII in the online-only Data Supplement). Serum aMrp-NP bound heparin in a dose-dependent manner suggesting that nanoparticles are able to retain heparin-binding properties in vivo.

Therapeutic Properties of aMrp-NPs in an In Vitro Model of Inflammation

Having demonstrated aMrp-NPs selectivity for certain populations of cells in plaques via MRI and flow-cytometric profiling, we further explored whether aMrp-NP can serve as

targeted therapeutics. Firstly, we tested recombinant Mrp8 and Mrp14 as inflammation-associated stimuli in BMDM under conditions indicated in Figure 6A. TNF-α concentration in the media was determined by ELISA to be ≈420-fold higher than control after 5 hours of stimulation with rMrp8/14. Polymyxin B pretreatment had no inhibitory effect on TNF-α release in recombinant Mrp8 and Mrp14 (rMrp8/14)-treated ApoE$^{-/-}$ BMDMs, whereas LPS-induced inflammation was abolished. No significant heating effects were observed for LPS, whereas complete inhibition was evident for Mrp8/14. Thus, LPS contamination is highly unlikely in both recombinant proteins in our possession. Different formulations (aMrp-NP, IgG-NP, or vehicle) were probed in activated BMDMs and a panel of inflammatory cytokines (TNF-α, IFN-γ, MCP-1, and IL-6) was analyzed in cell culture media after 5 hours of treatment. Inflammatory effects induced by either rMrp8 or rMrp14 or equal mixture of both were neutralized when aMrp-NP was added. No neutralization effect was observed with IgG-NP or sham control.

Discussion

In this work, we describe novel gadolinium containing designer nanoprobes displaying antibodies against Mrp-8/14 to target inflammation in a murine model of atherosclerosis. Molecular probes targeting atherosclerosis-associated moieties have been widely used in research settings.[16–19] The challenge has been to identify suitable ligands that simultaneously provide sufficient selectivity and high levels of expression and serve in a pathophysiologic context so that ligation of the target results in neutral or even beneficial effects on the disease process. Inflammation-associated “calgranulins,” S100A8 (Mrp8) and S100A9 (Mrp14) are upregulated following activation in response to cell contact with activated endothelium.[8,20,21] Mrp-14 forms a heterodimeric complex with Mrp-8 and is isolated almost exclusively in the dimeric form (Mrp).[1,3–5] Mrp-14 is functionally homologous across species, is highly expressed in atherosclerosis, and participates in amplification of inflammation, providing a compelling rationale for targeting this protein in translational studies.[22–24] Although Mrp-8/14 is cytoplasmic, it is secreted in response to inflammatory cell activation.[8] Mrp-8/14 is thus detected in the circulation, and a number of studies have corroborated its independent predictive value for events related to unstable plaque including acute coronary syndrome and stroke.[7,25] Once secreted extracellularly, the complex has been shown to bind to heparan and heparin sulfate glycosoaminoglycans (GAG) and activate inflammatory signaling cascades including toll-like receptor 4 (TLR4) and receptor for advanced glycation endproducts with downstream inflammatory cytokine release via NF-kappa B or FAT/CD36 dependent mechanisms.[6,13,26–28] Using Mrp-14$^{-/-}$ mice, we have demonstrated previously that Mrp-8/14 broadly regulates vascular inflammation in atherosclerosis and experimental angioplasty.[1,29,30] In order to test the in vivo efficacy of our approach, we used high-fat fed ApoE$^{-/-}$ mice with ApoE$^{-/-}$/Mrp14$^{-/-}$ serving as controls. Despite the presence of Mrp-8 mRNA transcripts, Mrp-14$^{-/-}$ mice lack both Mrp-8 and Mrp-14 protein due to the instability of Mrp-8 in the absence of Mrp-14.[1,31,32] Disruption of the Mrp-8/14 axis in the Mrp-14$^{-/-}$ mice enabled experimental testing of the specificity of our theranostic approach.

Macrophage targeting approaches have been used widely to image inflammation, particularly with MRI. The latter offers the advantage of superb soft tissue detail juxtaposed with safety and the advantage of using approved contrast agents conjugated to antibodies or ligands that recognize specific epitopes allowing preferential delivery to cell/tissue niches.[16,17,33] A related approach is to take advantage of functional properties of the macrophage such as phagocytosis to increase signal.[9,34,35] Apoptotic cell debris is ubiquitous in advanced atheroma with extensive evidence that apoptotic cell engulfment/removal by macrophages is facilitated by PS exteriorized on the surface of apoptotic cells.[36–41] Engulfment of PS has been shown in prior studies to diminish inflammatory

phenotype in macrophages.[42] Additional molecular cues such as oxidized phospholipids, derived from lipid peroxidation of fatty acids, may represent additional "eat-me" signals.[36,40,41]

In our approach to the design of multivalent theranostic nanoparticles we took advantage of a widely expressed lipid within foam cells (ω-carboxynonanoyl-cholesteryl ester) and PS, both to serve as an engulfment signals to engage macrophages for facilitated nanoparticle uptake.[43] Moreover, immunocoupling of anti-Mrp antibody to the surface of the nanoparticles offers their improved retention within plaques due to antigen binding. Thus, multivalent targeting of these NPs by 2 different, possibly synergistic mechanisms would increase targeted delivery of contrast media and/or therapeutics.

Maleimide-labeled PEG lipids were incorporated additionally into this formulation in order to prolong plasma half-life and enable immune-targeting. The probes were designed carrying a near infrared dye (AlexaFluor 647) as we envisioned potential difficulties in detection of plaque cell populations if stained with less photostable dyes. The T1 shortening effects of the nanoprobes thus synthesized were not substantially different from the Gd formulation that was incorporated. We anticipated potentiation of signal enhancement of the vessel wall, as a result of selective targeting of aMrp-NP to areas of vessel inflammation and accelerated phagocytosis by innate immune cells through high-efficiency mechanisms including scavenger receptor and integrin mediated pathways.[9,10] In keeping with our hypothesis, our experimental findings in vivo and uptake experiments performed in vivo provided corroborative evidence. Our in vivo experiments demonstrated that aMrp-NP nanoparticles accumulated in the pericellular space and extra cellular matrix supporting our targeting strategy. The in vitro data on the other hand provided evidence of rapid uptake by macrophages and accumulation in the lysosomal compartment.

The in vivo pharmacokinetics of the probe revealed relatively rapid clearance from the circulation in ApoE$^{-/-}$ mice but a relatively more prolonged clearance in DKO mice. As one would anticipate, the predominant locus of distribution was in the liver and spleen. In vivo vascular imaging studies demonstrated marked increase in vessel wall enhancement, consistent with the wide-expression of the Mrp8/14 in atherosclerosis.[1] The vessel wall imaging data were obtained at 24-hour post injection and suggest retention of the probe in the vessel wall. Flow cytometric profiling of plaque-derived cells demonstrated CD11b^{hi}, Ly6G^{hi}, and CD31^{+} cells as predominant cellular targets for aMrp-NP, confirming selective binding to monocytes, neutrophils, and endothelial cells, respectively. In additional confirmatory experiments involving cultured endothelial cells, we were able to demonstrate that Mrp in conditioned media derived from stimulated macrophages were indeed able to bind to the endothelial cell surface. These results are consistent with previous studies that have demonstrated that the Mrp-8/14 complex binds to endothelial cells via the Mrp-14 subunit, interacting chiefly with heparin, heparan sulfate, and chondroitin sulfate B GAGs. These 3 GAGs all contain significant amounts of iduronic acid, which is thought to be structurally important for many specific protein-GAG interactions. The interaction between heparin and heparin sulfate GAGs has high affinity (Kd 6.1±3.4 nmol/L) and is much higher than that reported for other proteins such as chemokines (RANTES and IL-8) (Kd in mM range).[44] This allows for preferential binding and sequestration of Mrp-8/14 in tissue niches with high content of these GAGs.[13] The precise locus of interaction between Mrp and GAGs has been speculated to involve tertiary structure of Mrp-8/14 as classic heparin binding consensus units are lacking in the monomers. Additional interactions of Mrp-8/14 with carboxylated N-glycans on endothelial cells have also been described that may be distinct from the GAG binding and this may additionally provide a concentration gradient of Mrp-8/14 expression and influence deposition of the protein in matrix areas rich in GAGs

and carboxyated N-glycans.[15] One may hypothesize that this interaction may allow prolonged retention of the probe and provide continuing therapeutic effects.

There are a number of important limitations that need to be considered and acknowledged in interpreting this work. We have not provided in vivo evidence of theranostic effect via reduction in plaque inflammation/size with treatment with our nanoparticles. Further experimentation will be needed to understand the long-term effects and whether this approach is successful in reducing atherosclerosis. The stability of the preparation in vivo may need further consideration, as it is entirely possible that despite PEG protection there could be disintegration of the particle resulting in leaching of the antibody and ultimate low tissue levels. Such an effect would however be difficult to monitor in vivo, and in the ultimate analysis only efficacy studies would allow us to make definitive conclusions. Another limitation is that the short circulation half-life of aMrp-NP may result in unfavorable pharmacodynamics. The increased clearance (short-$t_{1/2}$) may be explained by opsonization and uptake via Fc-mediated clearance by the reticuloendothelial system. The use of smaller fragments such as Fab' to prepare plaque-targeted nanoparticles could minimize this type of clearance. Our findings nonetheless have important implications for use of such an approach for the diagnosis and potential therapeutic modulation of inflammation in atherosclerosis.

Supplementary Material

Refer to Web version on PubMed Central for supplementary material.

Acknowledgments

We thank Yevgenia Tesmenitsky for help with the transgenic mice, and the Ohio State Campus Microscopy and Imaging Facility for their invaluable technical advice and assistance.

Sources of Funding This work was performed with support from National Heart, Lung, and Blood Institute Grant R21 HL106487. Dr Rajagopalan was partially supported by RO1 ES015146, R01ES017290, and R21 DK088522. Dr Maiseyeu was supported by American Heart Association Great Rivers Affiliate Postdoctoral Fellowship Program, award number 10POST4150090.

References

1. Croce K, Gao H, Wang Y, Mooroka T, Sakuma M, Shi C, Sukhova GK, Packard RR, Hogg N, Libby P, Simon DI. Myeloid-related protein-8/14 is critical for the biological response to vascular injury. Circulation. 2009; 120:427–436. [PubMed: 19620505]
2. Healy AM, Pickard MD, Pradhan AD, Wang Y, Chen Z, Croce K, Sakuma M, Shi C, Zago AC, Garasic J, Damokosh AI, Dowie TL, Poisson L, Lillie J, Libby P, Ridker PM, Simon DI. Platelet expression profiling and clinical validation of myeloid-related protein-14 as a novel determinant of cardiovascular events. Circulation. 2006; 113:2278–2284. [PubMed: 16682612]
3. Ostrand-Rosenberg S, Sinha P. Myeloid-derived suppressor cells: Linking inflammation and cancer. J Immunol. 2009; 182:4499–4506. [PubMed: 19342621]
4. Ryckman C, Vandal K, Rouleau P, Talbot M, Tessier PA. Proinflammatory activities of s100: proteins s100a8, s100a9, and s100a8/a9 induce neutrophil chemotaxis and adhesion. J Immunol. 2003; 170:3233–3242. [PubMed: 12626582]
5. Ionita MG, Vink A, Dijke IE, Laman JD, Peeters W, van der Kraak PH, Moll FL, de Vries JP, Pasterkamp G, de Kleijn DP. High levels of myeloid-related protein 14 in human atherosclerotic plaques correlate with the characteristics of rupture-prone lesions. ATVB. 2009; 29:1220–1227.
6. Hofmann MA, Drury S, Fu C, Qu W, Taguchi A, Lu Y, Avila C, Kambham N, Bierhaus A, Nawroth P, Neurath MF, Slattery T, Beach D, McClary J, Nagashima M, Morser J, Stern D, Schmidt AM. Rage mediates a novel proinflammatory axis: a central cell surface receptor for s100/calgranulin polypeptides. Cell. 1999; 97:889–901. [PubMed: 10399917]

7. Morrow DA, Wang Y, Croce K, Sakuma M, Sabatine MS, Gao H, Pradhan AD, Healy AM, Buros J, McCabe CH, Libby P, Cannon CP, Braunwald E, Simon DI. Myeloid-related protein 8/14 and the risk of cardiovascular death or myocardial infarction after an acute coronary syndrome in the pravastatin or atorvastatin evaluation and infection therapy: Thrombolysis in myocardial infarction (prove it-timi 22) trial. *American* Heart Journal. 2008; 155:49–55. [PubMed: 18082488]
8. Rammes A, Roth J, Goebeler M, Klempt M, Hartmann M, Sorg C. Myeloid-related protein (mrp) 8 and mrp14, calcium-binding proteins of the s100 family, are secreted by activated monocytes via a novel, tubulin-dependent pathway. *Journal of* Biological Chemistry. 1997; 272:9496–9502. [PubMed: 9083090]
9. Maiseyeu A, Mihai G, Roy S, Kherada N, Simonetti OP, Sen CK, Sun Q, Parthasarathy S, Rajagopalan S. Detection of macrophages via para-magnetic vesicles incorporating oxidatively tailored cholesterol ester: An approach for atherosclerosis imaging. Nanomedicine (Lond). 2010; 5:1341–1356. [PubMed: 21128718]
10. Maiseyeu A, Mihai G, Kampfrath T, Simonetti OP, Sen CK, Roy S, Rajagopalan S, Parthasarathy S. Gadolinium-containing phosphatidylserine liposomes for molecular imaging of atherosclerosis. *Journal of* Lipid Research. 2009; 50:2157–2163. [PubMed: 19017616]
11. Harel-Adar T, Ben Mordechai T, Amsalem Y, Feinberg MS, Leor J, Cohen S. Modulation of cardiac macrophages by phosphatidylserine-presenting liposomes improves infarct repair. Proc Natl Acad Sci USA. 2011; 108:1827–1832. [PubMed: 21245355]
12. Kampfrath T, Maiseyeu A, Ying Z, Shah Z, Deiuliis JA, Xu X, Kherada N, Brook RD, Reddy KM, Padture NP, Parthasarathy S, Chen LC, Moffatt-Bruce S, Sun Q, Morawietz H, Rajagopalan S. Chronic fine particulate matter exposure induces systemic vascular dysfunction via NADPH oxidase and TLR4 pathways. *Circulation* Research. 2011; 108:716–726. [PubMed: 21273555]
13. Robinson MJ, Tessier P, Poulsom R, Hogg N. The s100 family heterodimer, mrp-8/14, binds with high affinity to heparin and heparan sulfate glycosaminoglycans on endothelial cells. *Journal of* Biological Chemistry. 2002; 277:3658–3665. [PubMed: 11723110]
14. Averill MM, Barnhart S, Becker L, Li X, Heinecke JW, Leboeuf RC, Hamerman JA, Sorg C, Kerkhoff C, Bornfeldt KE. S100a9 differentially modifies phenotypic states of neutrophils, macrophages, and dendritic cells: implications for atherosclerosis and adipose tissue inflammation. Circulation. 2011; 123:1216–1226. [PubMed: 21382888]
15. Srikrishna G, Panneerselvam K, Westphal V, Abraham V, Varki A, Freeze HH. Two proteins modulating transendothelial migration of leukocytes recognize novel carboxylated glycans on endothelial cells. J Immunol. 2001; 166:4678–4688. [PubMed: 11254728]
16. Choudhury RP, Fisher EA. Molecular imaging in atherosclerosis, thrombosis, and vascular inflammation. ATVB. 2009; 29:983–991.
17. Owen DR, Lindsay AC, Choudhury RP, Fayad ZA. Imaging of atherosclerosis. *Annual* Review of Medicine. 2011; 62:25–40.
18. Ta HT, Prabhu S, Leitner E, Jia F, von Elverfeldt D, Jackson KE, Heidt T, Nair AK, Pearce H, von Zur Muhlen C, Wang X, Peter K, Hagemeyer CE. Enzymatic single-chain antibody tagging: A universal approach to targeted molecular imaging and cell homing in cardiovascular disease. *Circulation* Research. 2011; 109:365–373. [PubMed: 21700932]
19. McCarty OJ, Conley RB, Shentu W, Tormoen GW, Zha D, Xie A, Qi Y, Zhao Y, Carr C, Belcik T, Keene DR, de Groot PG, Lindner JR. Molecular imaging of activated von Willebrand factor to detect high-risk atherosclerotic phenotype. *J Am Coll Cardiol Cardiovascular* Imaging. 2010; 3:947–955.
20. Frosch M, Strey A, Vogl T, Wulffraat NM, Kuis W, Sunderkotter C, Harms E, Sorg C, Roth J. Myeloid-related proteins 8 and 14 are specifically secreted during interaction of phagocytes and activated endothelium and are useful markers for monitoring disease activity in pauciarticular-onset juvenile rheumatoid arthritis. *Arthritis and* Rheumatism. 2000; 43:628–637. [PubMed: 10728757]
21. Voganatsi A, Panyutich A, Miyasaki KT, Murthy RK. Mechanism of extracellular release of human neutrophil calprotectin complex. *Journal of* Leukocyte Biology. 2001; 70:130–134. [PubMed: 11435495]
22. Hirono K, Foell D, Xing Y, Miyagawa-Tomita S, Ye F, Ahlmann M, Vogl T, Futatani T, Rui C, Yu X, Watanabe K, Wanatabe S, Tsubata S, Uese K, Hashimoto I, Ichida F, Nakazawa M, Roth J,

Miyawaki T. Expression of myeloid-related protein-8 and -14 in patients with acute kawasaki disease. J Am Coll Cardiol. 2006; 48:1257–1264. [PubMed: 16979015]

23. McCormick MM, Rahimi F, Bobryshev YV, Gaus K, Zreiqat H, Cai H, Lord RS, Geczy CL. S100a8 and s100a9 in human arterial wall. Implications for atherogenesis. *Journal of* Biological Chemistry. 2005; 280:41521–41529. [PubMed: 16216873]
24. Nacken W, Sopalla C, Propper C, Sorg C, Kerkhoff C. Biochemical characterization of the murine s100a9 (mrp14) protein suggests that it is functionally equivalent to its human counterpart despite its low degree of sequence homology. *European* Journal of Biochemistry/FEBS. 2000; 267:560–565. [PubMed: 10632726]
25. Ionita MG, Catanzariti LM, Bots ML, de Vries JP, Moll FL, Kwan Sze S, Pasterkamp G, de Kleijn DP. High myeloid-related protein: 8/14 levels are related to an increased risk of cardiovascular events after carotid endarterectomy. *Stroke*; A Journal of Cerebral Circulation. 2010; 41:2010–2015.
26. Loser K, Vogl T, Voskort M, Lueken A, Kupas V, Nacken W, Klenner L, Kuhn A, Foell D, Sorokin L, Luger TA, Roth J, Beissert S. The toll-like receptor 4 ligands Mrp8 and Mrp14 are crucial in the development of autoreactive CD8+ t cells. *Nature* Medicine. 2010; 16:713–717.
27. Vogl T, Tenbrock K, Ludwig S, Leukert N, Ehrhardt C, van Zoelen MA, Nacken W, Foell D, van der Poll T, Sorg C, Roth J. Mrp8 and Mrp14 are endogenous activators of toll-like receptor 4, promoting lethal, endotoxin-induced shock. *Nature* Medicine. 2007; 13:1042–1049.
28. Kerkhoff C, Sorg C, Tandon NN, Nacken W. Interaction of S100A8/S100A9-arachidonic acid complexes with the scavenger receptor cd36 may facilitate fatty acid uptake by endothelial cells. Biochemistry. 2001; 40:241–248. [PubMed: 11141076]
29. Wang Y, Sakuma M, Chen Z, Ustinov V, Shi C, Croce K, Zago AC, Lopez J, Andre P, Plow E, Simon DI. Leukocyte engagement of platelet glycoprotein Ibalpha via the integrin MAC-1 is critical for the biological response to vascular injury. Circulation. 2005; 112:2993–3000. [PubMed: 16260637]
30. Zago AC, Simon DI, Wang Y, Sakuma M, Chen Z, Croce K, Ustinov V, Shi C, Martinez Filho EE. The importance of the interaction between leukocyte integrin mac-1 and platelet glycoprotein IB-α for leukocyte recruitment by platelets and for the inflammatory response to vascular injury. *Arquivos* Brasileiros de Cardiologia. 2008; 90:54–63. [PubMed: 18317641]
31. Hobbs JA, May R, Tanousis K, McNeill E, Mathies M, Gebhardt C, Henderson R, Robinson MJ, Hogg N. Myeloid cell function in Mrp-14 (S100A9) null mice. *Molecular and* Cellular Biology. 2003; 23:2564–2576. [PubMed: 12640137]
32. Manitz MP, Horst B, Seeliger S, Strey A, Skryabin BV, Gunzer M, Frings W, Schonlau F, Roth J, Sorg C, Nacken W. Loss of s100a9 (Mrp14) results in reduced interleukin-8-induced cd11b surface expression, a polarized microfilament system, and diminished responsiveness to chemoattractants in vitro. *Molecular and* Cellular Biology. 2003; 23:1034–1043. [PubMed: 12529407]
33. Choudhury RP, Fuster V, Badimon JJ, Fisher EA, Fayad ZA. MRI and characterization of atherosclerotic plaque: Emerging applications and molecular imaging. *Arteriosclerosis*, Thrombosis, and Vascular Biology. 2002; 22:1065–1074.
34. Libby P, Nahrendorf M, Weissleder R. Molecular imaging of atherosclerosis: A progress report. *Texas Heart Institute* Journal. 2010; 37:324–327. [PubMed: 20548813]
35. van Schooneveld MM, Vucic E, Koole R, Zhou Y, Stocks J, Cormode DP, Tang CY, Gordon RE, Nicolay K, Meijerink A, Fayad ZA, Mulder WJ. Improved biocompatibility and pharmacokinetics of silica nanoparticles by means of a lipid coating: a multimodality investigation. *Nano* Letters. 2008; 8:2517–2525. [PubMed: 18624389]
36. Ravichandran KS, Lorenz U. Engulfment of apoptotic cells: signals for a good meal. *Nature* Reviews Immunology. 2007; 7:964–974.
37. Podrez EA, Poliakov E, Shen Z, Zhang R, Deng Y, Sun M, Finton PJ, Shan L, Febbraio M, Hajjar DP, Silverstein RL, Hoff HF, Salomon RG, Hazen SL. A novel family of atherogenic oxidized phospholipids promotes macrophage foam cell formation via the scavenger receptor cd36 and is enriched in atherosclerotic lesions. *Journal of* Biological Chemistry. 2002; 277:38517–38523. [PubMed: 12145296]

38. Huynh ML, Fadok VA, Henson PM. Phosphatidylserine-dependent ingestion of apoptotic cells promotes tgf-beta1 secretion and the resolution of inflammation. *Journal of* Clinical Investigation. 2002; 109:41–50. [PubMed: 11781349]
39. Hazen SL. Oxidized phospholipids as endogenous pattern recognition ligands in innate immunity. *Journal of* Biological Chemistry. 2008; 283:15527–15531. [PubMed: 18285328]
40. Greenberg ME, Li XM, Gugiu BG, Gu X, Qin J, Salomon RG, Hazen SL. The lipid whisker model of the structure of oxidized cell membranes. *Journal of* Biological Chemistry. 2008; 283:2385–2396. [PubMed: 18045864]
41. Greenberg ME, Sun M, Zhang R, Febbraio M, Silverstein R, Hazen SL. Oxidized phosphatidylserine-cd36 interactions play an essential role in macrophage-dependent phagocytosis of apoptotic cells. *Journal of* Experimental Medicine. 2006; 203:2613–2625. [PubMed: 17101731]
42. Ramos GC, Fernandes D, Charao CT, Souza DG, Teixeira MM, Assreuy J. Apoptotic mimicry: Phosphatidylserine liposomes reduce inflammation through activation of peroxisome proliferator-activated receptors (PPARS) in vivo. *British* Journal of Pharmacology. 2007; 151:844–850. [PubMed: 17533418]
43. Li AC, Glass CK. The macrophage foam cell as a target for therapeutic intervention. *Nature* Medicine. 2002; 8:1235–1242.
44. Kuschert GS, Coulin F, Power CA, Proudfoot AE, Hubbard RE, Hoogewerf AJ, Wells TN. Glycosaminoglycans interact selectively with chemokines and modulate receptor binding and cellular responses. Biochemistry. 1999; 38:12959–12968. [PubMed: 10504268]

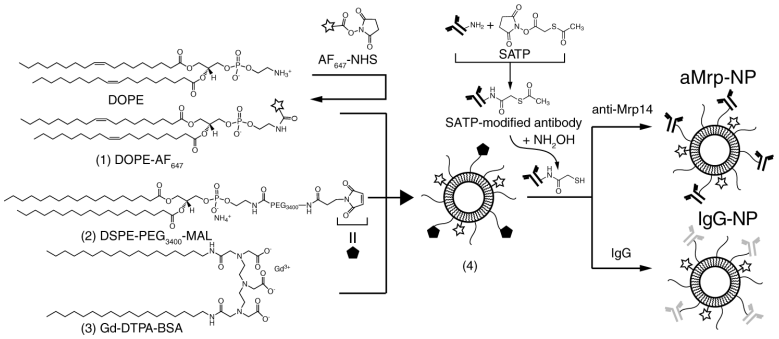

Figure 1.

Synthesis of antibody-decorated nanoparticles. AlexaFluor 647 (AF647)-tagged lipids (1) as well as gadolinium lipids (3) were synthetized. Nanoparticles were then formed with maleimide polyethylene glycol (PEG) lipids (2), PEG lipids, ω-carboxynonanoylcholesteryl ester, and phosphatidylserine (not shown). Nanoparticles (4) were subsequently conjugated with polyclonal anti-myeloid-related protein (Mrp)-14 or nonspecific IgG antibodies via maleimide-sulfhydryl chemistry.

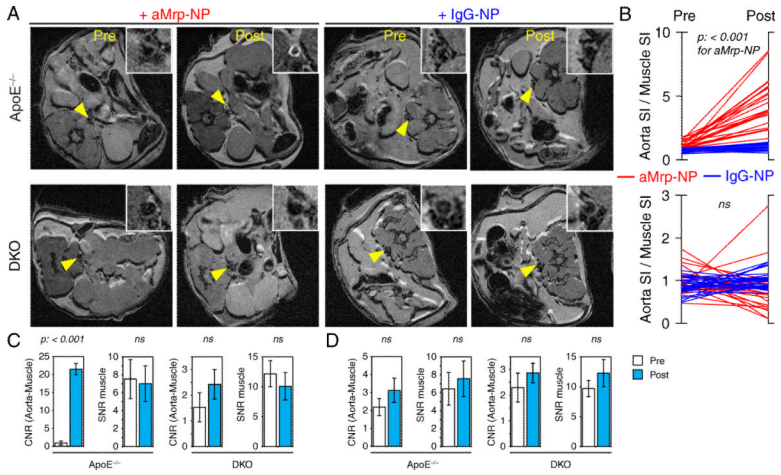

Figure 2.

Myeloid-related protein (Mrp)-targeted paramagnetic nanoparticles enhanced signal of atherosclerotic aortas in ApoE$^{-/-}$ mice. **A**, Representative T1 weighted axial images with **arrows** indicating abdominal aorta (magnified in insets) of ApoE$^{-/-}$ and ApoE$^{-/-}$/Mrp14$^{-/-}$ (double knockout [DKO]) mice before and 24 hours after the injection of anti-Mrp14 nanoprobes (aMrp-NP) or IgG-NP. **B**, aMrp-NP but not nonspecific IgG-conjugated gadolinium nanoprobe (IgG-NP) administration produced a statistically significant increase of aorta SI/muscle SI in ApoE$^{-/-}$. One-way repeated-measures ANOVA was performed by comparing intensity of 48 pixels in pre- and postinjection images. **C**, A significant increase in aorta-muscle contrast-to-noise ratio (CNR) 24 hours after aMrp-NP injection was found in the ApoE$^{-/-}$ but not the DKO group. **D**, IgG-NP administration did not produce an increase in CNR.

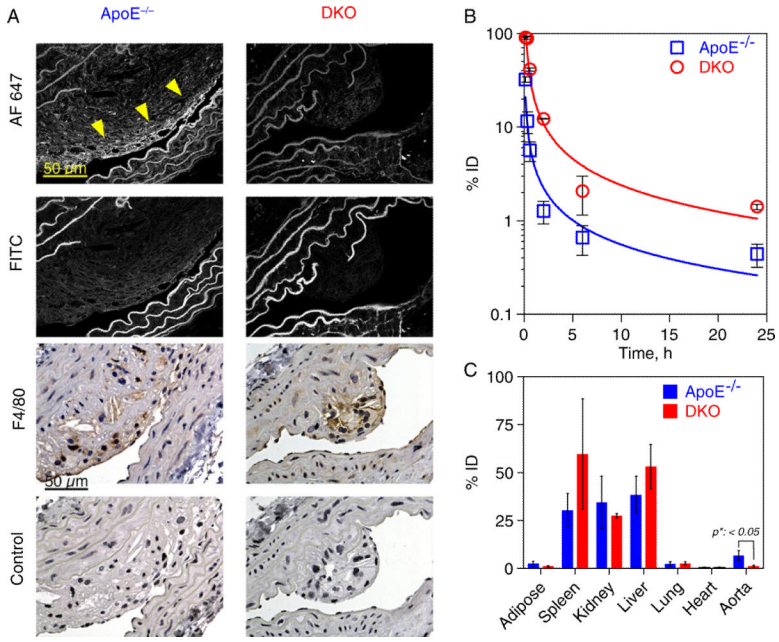

Figure 3.

Histological, pharmacokinetic and biodistribution evaluation of anti-Mrp14 nanoprobes (aMrp-NP) in ApoE$^{-/-}$ or double knockout (DKO) mice post intravenous administration. **A**, Histological validation of MRI data on the presence of aMrp-NP in plaque (AF647 signal indicated by **arrowheads**). **B**, aMrp-NP displayed a prolonged circulation time in the blood of DKO animals compared to ApoE$^{-/-}$ mice. **C**, The concentration of aMrp-NP was determined based on Gd content found in different organs by ICP-MS, normalized per gram dry weight of tissue and expressed as percent of injected dose (%ID).

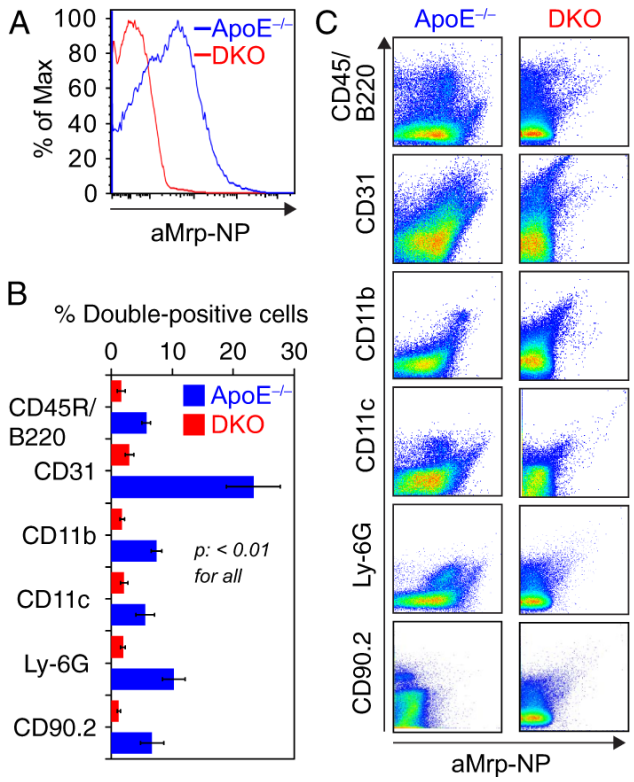

Figure 4.

Flow-cytometric screening of digested aortas from ApoE$^{-/-}$ and double knockout (DKO) animals showing relative uptake of anti-Mrp14 nanoprobes (aMrp-NP) by different cell types. Aortas were digested in an enzyme cocktail and the resulting cell suspension was labeled with fluorescent antibodies to enable analysis of aMrp-NP content in B-cells (CD45/B220), endothelial cells (CD31), monocytes/macrophages (CD11b), dendritic cells (CD11c), neutrophils (Ly-6G), and T-cells (CD90.2). **A**, Histogram for total cells labeled with aMrp-NP-derived AlexaFluor 647 showed increased fluorescence intensity in ApoE$^{-/-}$ cells. **B**, FACS analysis demonstrated significantly higher aMrp-NP uptake by CD31^{+}, CD11b^{+}, CD11c^{+}, and Ly-6G^{+} cells in ApoE$^{-/-}$ group; n=5 to 7. **C**, Representative dot plots of cell marker vs. AlexaFluor 647-gated cells.

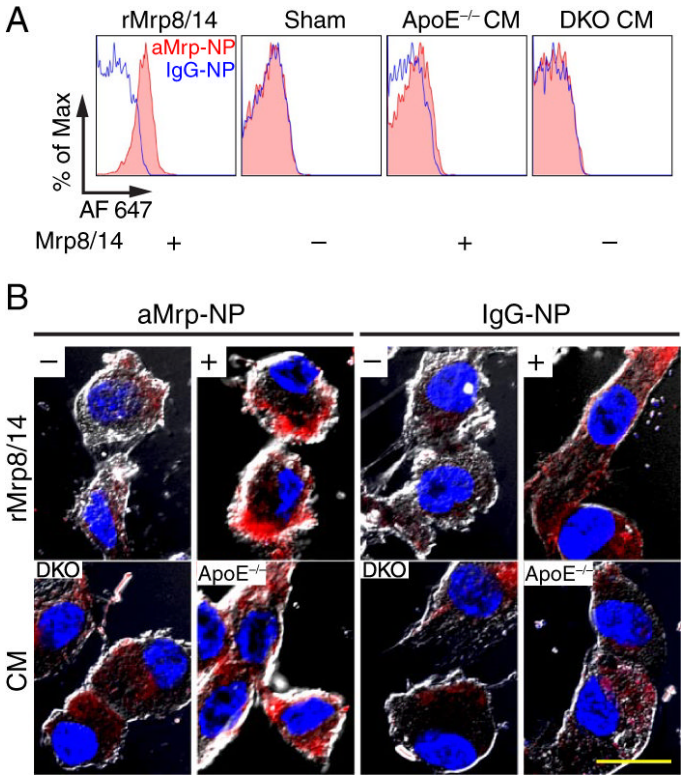

Figure 5.

Anti-Mrp14 nanoprobes (aMrp-NPs) bind to endothelial cells displaying exogenous Mrps on the surface. Human umbilical vein endothelial cells (HUVECs) were pretreated with either rMrp8/14 or sham (phosphate-buffered saline), or cultured in the presence of cell-conditioned media (CM) of LPS-activated bone marrow derived macrophages (BMDMs). BMDMs were cultured from ApoE$^{-/-}$ (Mrp+) or double knockout (DKO) (Mrp−) mice. Pretreated HUVECs were then exposed to aMrp-NP (red, filled histograms) or IgG-NP (blue, open histograms) at +4°C cells were washed and subjected to (**A**) FACS analysis or (**B**) were imaged by confocal microscopy. Confocal microscopy micrographs are a composite of AlexaFluor 647 fluorescence (red, aMrp-NP) and bright-field images. Nuclei were stained with DAPI (blue). The bar represents 20 μm.

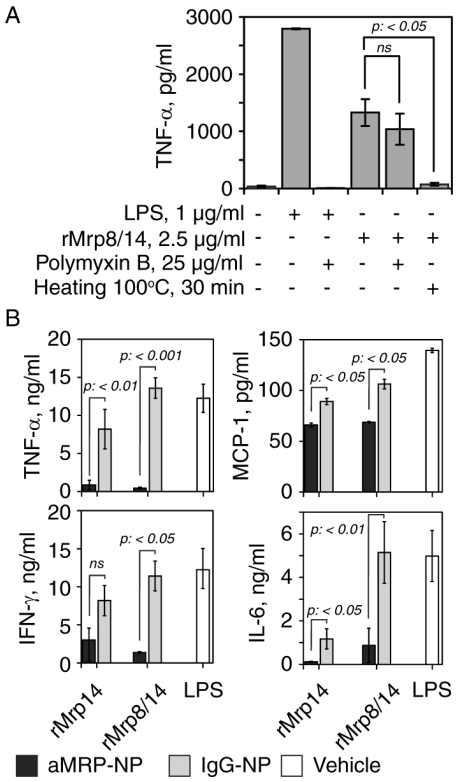

Figure 6.

Anti-Mrp14 nanoprobe (aMrp-NP) was able to abolish inflammatory effects in vitro. **A**, Heating but not pretreatment with Polymyxin B had inhibitory effects on TNF-α release by rMrp-stimulated mouse bone marrow derived macrophages (BMDM). The effects of LPS were abolished by Polymyxin B. **B**, aMrp-NP but not nonspecific IgG-conjugated gadolinium nano-probe (IgG-NP) was able to neutralize the inflammatory effects of rMrp-14 or mixture of rMrp-8 and rMrp-14 on BMDM. LPS-treated cells with phosphate-buffered saline vehicle served as a positive control. The mean data represent 3 separate experiments. IFN indicates interferon; IL, interleukin.